

Modeling double bounded data based on correlated gamma random variables

Roberto Vila^{1*}, Felipe Quintino¹ and Marcelo Bourguignon²

¹ *Department of Statistics, University of Brasilia, Brasilia, Brazil*

² *Department of Statistics, Federal University of Rio Grande do Norte, Natal, RN, Brazil*

March 4, 2026

Abstract

Many types of bounded data defined on the unit interval arise naturally as ratios of the form $X/(X + Y)$. In the existing literature, the main statistical models proposed for this type of bounded data typically based on the assumption that the random variables X and Y are independent. However, this assumption is often unrealistic in practical applications, where X and Y tend to be correlated due to shared underlying mechanisms or common sources of variability. In this paper, we overcome such limitations and propose a model in which the marginal distributions of the two components are linked by a copula, leading to a more flexible and realistic representation of unit-interval data. In particular, in the proposed model, X and Y are correlated gamma random variables linked by the Farlie-Gumbel-Morgenstern (FGM) copula, allowing for positive and negative correlations between the components. The mathematical properties and practical applications are rigorously investigated. Depending on the choice of parameters, the new model is very versatile, showing symmetric or asymmetric behavior, as well as unimodality or bimodality. A Monte Carlo simulation study is carried out that shows the good performance of the maximum likelihood estimator in several scenarios of parameter choices. The potential and limitations of efficient likelihood-based computations are also discussed. We evaluate the effectiveness of the new model and its estimates in modeling real-world datasets related to economics.

Keywords. Extended beta distribution · Morgenstern's bivariate distribution · Monte Carlo simulation · R software.
Mathematics Subject Classification (2010). MSC 60E05 · MSC 62Exx · MSC 62Fxx.

1 Introduction

Several natural indicators are measured as indicators, percentages, proportions, ratios, and rates that are bounded on a certain interval, usually in the bounded interval $(0, 1)$. The need for modeling and analyzing bounded data occurs in many fields of real life such as the Human Development Index, COVID-19 recovery

*Corresponding author: Roberto Vila, email: rovig161@gmail.com

rates, and percentages, among others. Certainly, the two parameter beta distribution is the most common distribution used in the literature to describe data in the unit interval, especially because of its flexibility.

Malik (1967) and Ahuja (1969) both showed that if X and Y are independent random variables following gamma distributions with shape parameters $\alpha > 0$ and $\beta > 0$, and the same scale parameter σ , i.e., $X \sim \text{GA}(\alpha, \sigma)$ and $Y \sim \text{GA}(\beta, \sigma)$, then

$$Z \stackrel{d}{=} \frac{Z}{X + Y} \sim \text{Beta}(\alpha, \beta), \quad (1)$$

namely, Z is beta distributed with shape parameters $\alpha, \beta > 0$ and $\stackrel{d}{=}$ stands for equality in distribution. It should be noted that stochastic representations are important since they may justify some models arising naturally in real situations. Furthermore, models generated by (1) can produce distributions with different shapes, such as symmetry, bimodality, and others. This allows estimation procedures to better capture the inherent structures in the data. However, the independence assumption seems to be not suitable in real situations, where we would expect a relationship between these variables. The case of positively correlated gamma distributed components has earlier been studied by Nadarajah and Kotz (2006) based on the Kibble bivariate gamma distribution for (X, Y) (Kibble, 1941). However, negatively correlated measurements are encountered in numerous applications, for example in COVID-19 recovery rates, where X and Y are two random variables representing the number of confirmed COVID-19-related deaths and COVID-19 cases without death result, and the independence assumption seems to be not suitable in this case.

In this context, considering distributed components negatively and positively correlated, and satisfying the stochastic representation in (1), Vila et al. (2024b) proposed a class of unit-log-symmetric models to analyzing an internet access data. Vila et al. (2025) introduced a new distribution in the unit interval where X and Y are two correlated Birnbaum-Saunders random variables. In the same way, Vila and Quintino (2026) considered a novel unit-asymmetric distribution, where X and Y are two correlated Fréchet random variables.

In this work, following the same stochastic formulation as the beta distribution, we introduce a new class of unit models that arises from a ratio (1) of two correlated gamma random variables. We consider (X, Y) distributed as Morgenstern's bivariate distribution with gamma margins (cf. Lai, 1978). The new model extends the well-known Beta distribution with the addition of one parameter. However, this extra parameter makes the model able to exhibit U- or J-shapes, symmetry, and bimodality. Moreover, information criteria on real-world dataset applications show that better fits are obtained with the new model, even with this extra parameter. Maximum likelihood based estimation procedures are discussed for the new distribution. A Monte Carlo simulation study is carried out, as well as applications to datasets well-consolidated in the literature, showing the versatility of the new model. Our results rely on special functions and their properties, which let us explicitly derive the probability density function (PDF), the cumulative distribution function (CDF), and key characteristics of the new probabilistic model. Special functions are widely studied because they encompass many classes of functions and provide useful identities for integration, differentiation, and other operations. Some well-known examples are the Gauss hypergeometric ${}_2F_1$ function, Meijer's G -function, Fox's H -function, modified Bessel K_ν -function of the 3rd kind (see Definitions 1.1, 1.5 and 1.6 and 1.11 in Mathai et al., 2010), and the double hypergeometric Appel functions F_1, F_2, F_3 and F_4 (Appell, 1925).

The remainder of this paper is organized as follows: Section 2 introduces the new model and plots of its shape for different parameter choices. Section 3 deals with the derivation of the new unit distribution and its mathematical properties, such as symmetry, stochastic representation, characterization as a ratio and

moments. In Section 4, we propose the estimation of the parameters. In Section 5, we discuss Monte Carlo simulations to evaluate the proposed estimator, its computational challenges, and alternative frameworks. In Section 6, we address modeling real-world scenarios involving an income consumption dataset. The final section presents our conclusions.

2 The extended beta distribution

We say that an absolutely continuous random variable Z , with support $(0, 1)$, follows an extended bimodal beta (EBB) distribution with parameter vector $\theta = (\alpha, \beta, \rho)^\top$, $\alpha > 0$, $\beta > 0$, and $-1 \leq \rho \leq 1$, denoted by $Z \sim \text{EBB}(\theta)$, if its PDF is given by (for $0 < z < 1$)

$$\begin{aligned}
f_Z(z; \theta) &= (1 + \rho) \frac{z^{\alpha-1} (1-z)^{\beta-1}}{B(\alpha, \beta)} \\
&\quad - \frac{2\rho\Gamma(2\alpha + \beta)}{\alpha\Gamma^2(\alpha)\Gamma(\beta)} \frac{z^{2\alpha-1} (1-z)^{\beta-1}}{(1+z)^{2\alpha+\beta}} {}_2F_1\left(1, 2\alpha + \beta; 1 + \alpha; \frac{z}{1+z}\right) \\
&\quad - \frac{2\rho\Gamma(\alpha + 2\beta)}{\beta\Gamma(\alpha)\Gamma^2(\beta)} \frac{z^{\alpha-1} (1-z)^{2\beta-1}}{(2-z)^{\alpha+2\beta}} {}_2F_1\left(1, \alpha + 2\beta; 1 + \beta; \frac{1-z}{2-z}\right) \\
&\quad + \frac{4^{1-\alpha-\beta}\rho\Gamma(2\alpha + 2\beta)}{\alpha\beta\Gamma^2(\alpha)\Gamma^2(\beta)} z^{2\alpha-1} (1-z)^{2\beta-1} F_2\left(2\alpha + 2\beta, 1, 1; \alpha + 1, \beta + 1; \frac{z}{2}, \frac{1-z}{2}\right), \quad (2)
\end{aligned}$$

where $\Gamma(\alpha) = \int_0^\infty t^{\alpha-1} \exp(-t) dt$ is the complete gamma function, $B(\alpha_1, \alpha_2) = \Gamma(\alpha_1)\Gamma(\alpha_2)/\Gamma(\alpha_1 + \alpha_2)$ is the complete beta function,

$${}_2F_1(a, b; c; x) = \sum_{n=0}^{\infty} \frac{(a)_n (b)_n x^n}{(c)_n n!}$$

is the hypergeometric function,

$$F_2(a, b_1, b_2; c_1, c_2; x, y) = \sum_{m,n=0}^{\infty} \frac{(a)_{m+n} (b_1)_m (b_2)_n x^m y^n}{(c_1)_m (c_2)_n m! n!} \quad (3)$$

denotes the Appell F2 double hypergeometric function, and $(q)_n = \Gamma(q + n)/\Gamma(q)$ is the Pochhammer symbol. Conditions for the convergence of the series and several properties of these special functions are given in [Mathai et al. \(2010\)](#) and [Ananthanarayan et al. \(2023\)](#).

Remark 2.1. Note that when $\rho = 0$ the EBB model in (2) becomes the classic beta distribution. Therefore, the EBB model can be interpreted as a new extended bimodal beta distribution.

Figure 1 shows the PDF $f_Z(z)$ behavior for some parameter choices. Note that we can have a symmetric distribution centered around 0.5 (if $\alpha = \beta$, see Figure 2). It is also possible to obtain asymmetric or bimodal (Figure 3) models, depending on the choice of parameters.

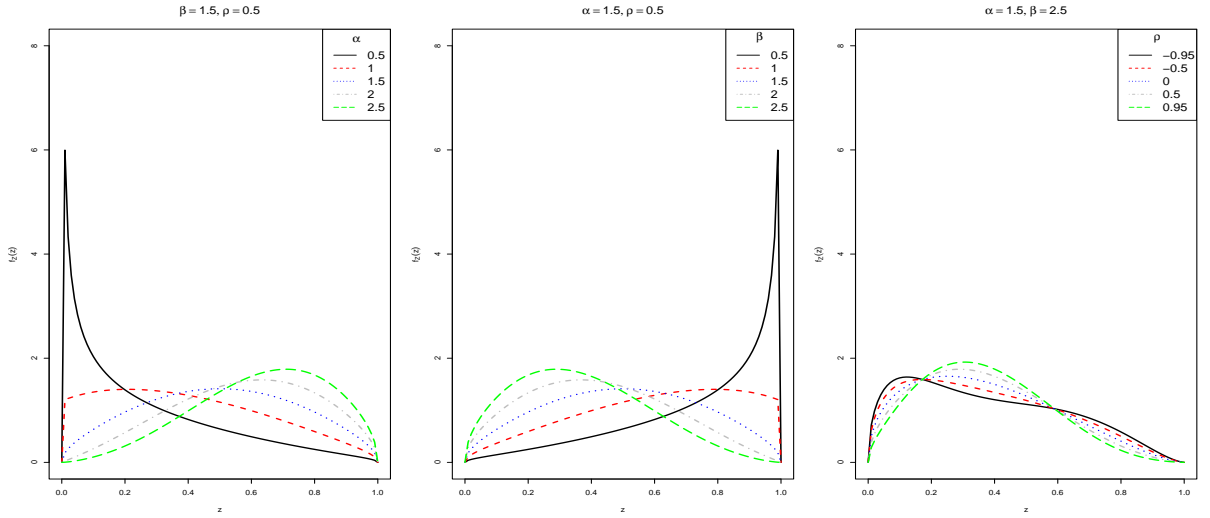


Figure 1: Plot of the PDF f_Z with varying parameters α (left), β (middle) and ρ (right).

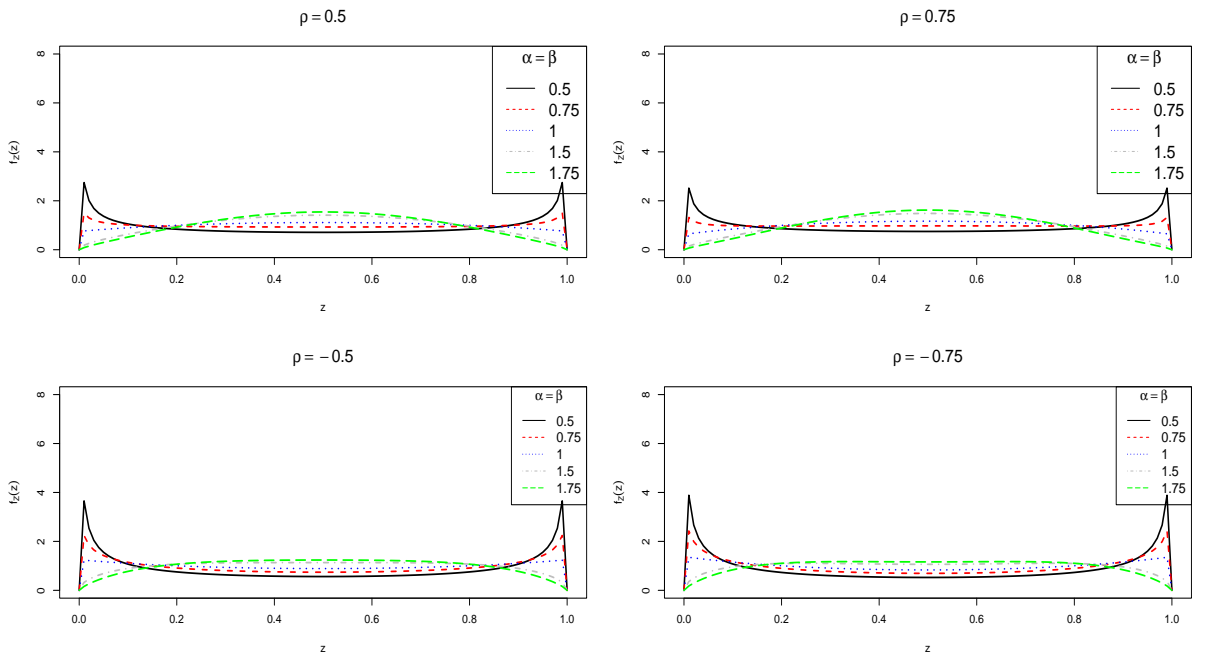


Figure 2: Plot of the PDF f_Z with varying parameters $\alpha = \beta$ for $\rho \in \{-0.5, -0.75, 0.5, 0.75\}$.

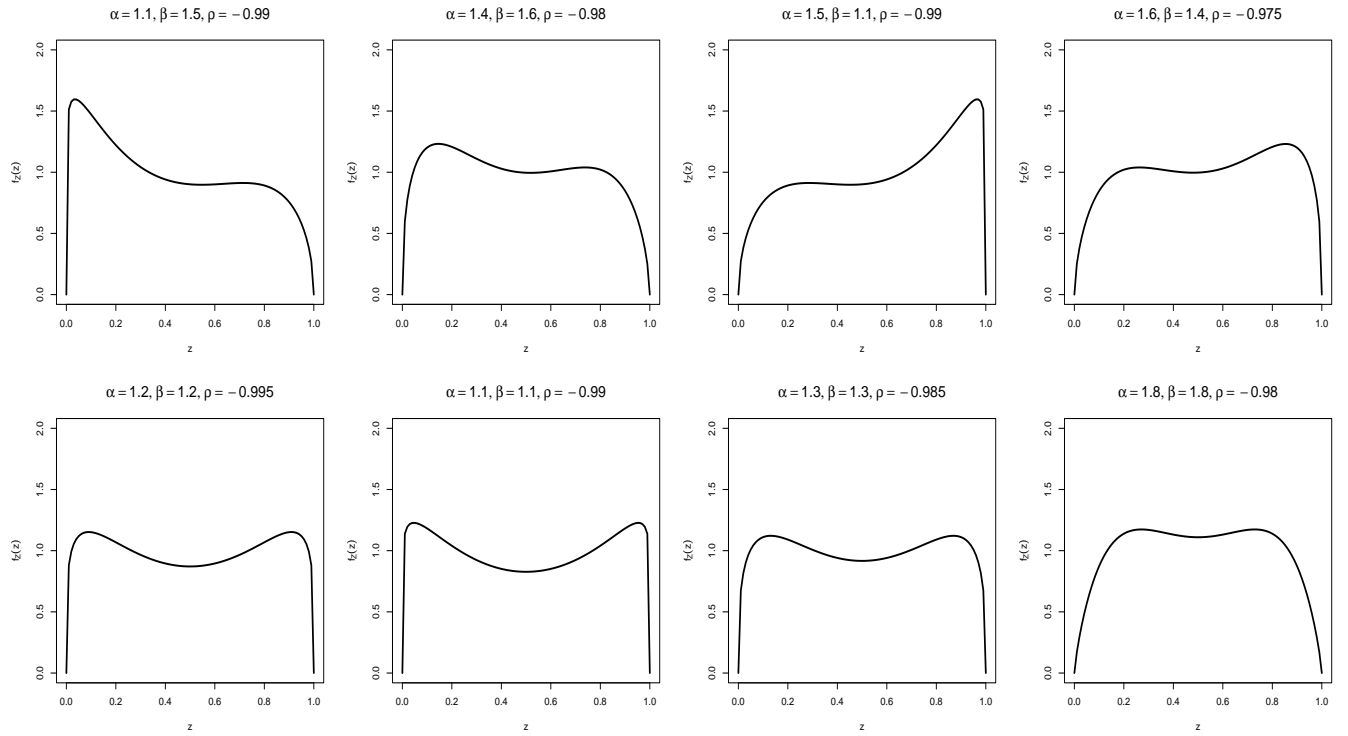


Figure 3: Plot of the PDF f_Z with varying parameters α , β and ρ , illustrating bimodality.

In Figures 1–3 we note that:

- for $\alpha > \beta$, the shapes are concentrated on the right side of the interval $[0, 1]$;
- for $\alpha < \beta$, the concentration is in the left side;
- when $\rho \approx -1$, bimodality can be observed. However, the two modes are not completely separated. After the first mode, the frequency does not drop near zero before rising again toward the second mode.

Remark 2.2. Usual techniques for establishing unimodality or bimodality rely on analyzing the sign of the PDF's derivative and its roots (see, e.g., Theorem 2.1 in Vila et al., 2024a). However, the PDF (2) involves the special functions ${}_2F_1$ and F_2 , which can make root analysis either impossible or extremely difficult from an analytical approach. The parameters shown in Figure 3 were selected after several rounds of testing and refinement.

3 Some basic properties

In this section we establish some basic mathematical properties of the extended bimodal beta distribution.

3.1 Symmetry

Let $Z \sim \text{EBB}(\boldsymbol{\theta})$. A simple observation shows that (for $0 < w < 1/2$)

$$\begin{aligned}
f_Z(z; \boldsymbol{\theta}) \Big|_{z=\frac{1}{2}-w} &= (1 + \rho) \frac{(\frac{1}{2} - w)^{\alpha-1} (\frac{1}{2} + w)^{\beta-1}}{\mathbf{B}(\alpha, \beta)} \\
&- \frac{2\rho\Gamma(2\alpha + \beta)}{\alpha\Gamma^2(\alpha)\Gamma(\beta)} \frac{(\frac{1}{2} - w)^{2\alpha-1} (\frac{1}{2} + w)^{\beta-1}}{(\frac{3}{2} - w)^{2\alpha+\beta}} {}_2F_1 \left(1, 2\alpha + \beta; 1 + \alpha; \frac{1 - 2w}{3 - 2w} \right) \\
&- \frac{2\rho\Gamma(\alpha + 2\beta)}{\beta\Gamma(\alpha)\Gamma^2(\beta)} \frac{(\frac{1}{2} - w)^{\alpha-1} (\frac{1}{2} + w)^{2\beta-1}}{(\frac{3}{2} + w)^{\alpha+2\beta}} {}_2F_1 \left(1, \alpha + 2\beta; 1 + \beta; \frac{1 + 2w}{3 + 2w} \right) \\
&+ \frac{4^{1-\alpha-\beta}\rho\Gamma(2\alpha + 2\beta)}{\alpha\beta\Gamma^2(\alpha)\Gamma^2(\beta)} \left(\frac{1}{2} - w \right)^{2\alpha-1} \left(\frac{1}{2} + w \right)^{2\beta-1} F_2 \left(2\alpha + 2\beta, 1, 1; \alpha + 1, \beta + 1; \frac{1 - 2w}{4}, \frac{1 + 2w}{4} \right) \quad (4)
\end{aligned}$$

and

$$\begin{aligned}
f_Z(z; \boldsymbol{\theta}) \Big|_{z=\frac{1}{2}+w} &= (1 + \rho) \frac{(\frac{1}{2} + w)^{\alpha-1} (\frac{1}{2} - w)^{\beta-1}}{\mathbf{B}(\alpha, \beta)} \\
&- \frac{2\rho\Gamma(2\alpha + \beta)}{\alpha\Gamma^2(\alpha)\Gamma(\beta)} \frac{(\frac{1}{2} + w)^{2\alpha-1} (\frac{1}{2} - w)^{\beta-1}}{(\frac{3}{2} + w)^{2\alpha+\beta}} {}_2F_1 \left(1, 2\alpha + \beta; 1 + \alpha; \frac{1 + 2w}{3 + 2w} \right) \\
&- \frac{2\rho\Gamma(\alpha + 2\beta)}{\beta\Gamma(\alpha)\Gamma^2(\beta)} \frac{(\frac{1}{2} + w)^{\alpha-1} (\frac{1}{2} - w)^{2\beta-1}}{(\frac{3}{2} - w)^{\alpha+2\beta}} {}_2F_1 \left(1, \alpha + 2\beta; 1 + \beta; \frac{1 - 2w}{3 - 2w} \right) \\
&+ \frac{4^{1-\alpha-\beta}\rho\Gamma(2\alpha + 2\beta)}{\alpha\beta\Gamma^2(\alpha)\Gamma^2(\beta)} \left(\frac{1}{2} + w \right)^{2\alpha-1} \left(\frac{1}{2} - w \right)^{2\beta-1} F_2 \left(2\alpha + 2\beta, 1, 1; \alpha + 1, \beta + 1; \frac{1 + 2w}{4}, \frac{1 - 2w}{4} \right). \quad (5)
\end{aligned}$$

As the the Appell F_2 double hypergeometric function is symmetric, that is, $F_2(a, b_1, b_2; c_1, c_2; x, y) = F_2(a, b_1, b_2; c_1, c_2; y, x)$, by taking $\alpha = \beta$ in the identities (4) and (5), we have (for $0 < w < 1/2$)

$$f_Z(z; \boldsymbol{\theta}) \Big|_{z=\frac{1}{2}-w} = f_Z(z; \boldsymbol{\theta}) \Big|_{z=\frac{1}{2}+w}.$$

That is, the EBB PDF in (2) is symmetric around $z_0 = 1/2$ provided $\alpha = \beta$ (see Figure 2). Moreover, in this case, the median and the mean of a EBB distribution both occur at $z_0 = 1/2$.

3.2 EBB model arising as a ratio of correlated random variables

In this subsection, we establish a fundamental property of the EBB model, in which the random variable Z in (2) is represented as a ratio of the form

$$Z \stackrel{d}{=} \frac{X}{X + Y}, \quad (6)$$

where $\stackrel{d}{=}$ means equality in distribution and the random vector $(X, Y)^\top$ follows a Morgenstern's bivariate distribution (with gamma margins) (Lai, 1978).

Following [Lai \(1978\)](#), a random vector $(X, Y)^\top$ has a Morgenstern's bivariate distribution if its cumulative distribution function (CDF) is of the form

$$F_{X,Y}(x, y) = F_X(x)F_Y(y)[1 + \rho\{1 - F_X(x)\}\{1 - F_Y(y)\}], \quad -1 \leq \rho \leq 1, \quad (7)$$

having $F_X(x)$ and $F_Y(y)$ as marginal distribution functions. It is clear that the corresponding joint PDF of $(X, Y)^\top$ is given by

$$f_{X,Y}(x, y) = f_X(x)f_Y(y)[1 + \rho\{2F_X(x) - 1\}\{2F_Y(y) - 1\}]. \quad (8)$$

Note that when $\rho = 0$, X and Y are independent.

In what follows, we verify that the random variable Z in (2) satisfies the stochastic representation (6), where $(X, Y)^\top$ has Morgenstern's bivariate distribution (7)-(8), and X and Y have gamma distributions with the same rate, more precisely, $X \sim \text{Gamma}(\alpha, \theta)$ and $Y \sim \text{Gamma}(\beta, \theta)$, $\alpha > 0, \beta > 0, \theta > 0$.

By fact, using the Jacobian method, we have (for $s = 1/z - 1$ and $0 < z < 1$)

$$f_{\frac{X}{X+Y}}(z) = (s+1)^2 \int_0^\infty x f_{X,Y}(x, sx) dx.$$

Using (8) in the above identity, we have the following

$$\begin{aligned} f_{\frac{X}{X+Y}}(z) &= (1+\rho)(s+1)^2 \int_0^\infty x f_X(x) f_Y(sx) dx - 2\rho(s+1)^2 \int_0^\infty [x f_X(x) f_Y(sx)] F_X(x) dx \\ &\quad - 2\rho(s+1)^2 \int_0^\infty [x f_X(x) f_Y(sx)] F_Y(sx) dx + 4\rho(s+1)^2 \int_0^\infty [x f_X(x) f_Y(sx)] F_X(x) F_Y(sx) dx \\ &\equiv (1+\rho)K_1(z) - \rho K_2(z) - \rho K_3(z) + \rho K_4(z), \end{aligned} \quad (9)$$

where

$$\begin{aligned} K_1(z) &\equiv (s+1)^2 \int_0^\infty x f_X(x) f_Y(sx) dx, \\ K_2(z) &\equiv 2(s+1)^2 \int_0^\infty [x f_X(x) f_Y(sx)] F_X(x) dx, \\ K_3(z) &\equiv 2(s+1)^2 \int_0^\infty [x f_X(x) f_Y(sx)] F_Y(sx) dx, \\ K_4(z) &\equiv 4(s+1)^2 \int_0^\infty [x f_X(x) f_Y(sx)] F_X(x) F_Y(sx) dx. \end{aligned} \quad (10)$$

Since $X \sim \text{Gamma}(\alpha, \theta)$, $Y \sim \text{Gamma}(\beta, \theta)$ and

$$x f_X(x; \alpha, \theta) f_Y(sx; \beta, \theta) = \frac{\theta^{\alpha+\beta} s^{\beta-1}}{\Gamma(\alpha)\Gamma(\beta)} x^{\alpha+\beta-1} \exp[-(1+s)\theta x],$$

we have

$$\begin{aligned}
K_1(z) &= (s+1)^2 \frac{\theta^{\alpha+\beta} s^{\beta-1}}{\Gamma(\alpha)\Gamma(\beta)} \int_0^\infty x^{\alpha+\beta-1} \exp[-(1+s)\theta x] dx, \\
K_2(z) &= 2(s+1)^2 \frac{\theta^{\alpha+\beta} s^{\beta-1}}{\Gamma^2(\alpha)\Gamma(\beta)} \int_0^\infty x^{\alpha+\beta-1} \exp[-(1+s)\theta x] \gamma(\alpha, \theta x) dx, \\
K_3(z) &= 2(s+1)^2 \frac{\theta^{\alpha+\beta} s^{\beta-1}}{\Gamma(\alpha)\Gamma^2(\beta)} \int_0^\infty x^{\alpha+\beta-1} \exp[-(1+s)\theta x] \gamma(\beta, \theta s x) dx, \\
K_4(z) &= 4(s+1)^2 \frac{\theta^{\alpha+\beta} s^{\beta-1}}{\Gamma^2(\alpha)\Gamma^2(\beta)} \int_0^\infty x^{\alpha+\beta-1} \exp[-(1+s)\theta x] \gamma(\alpha, \theta x) \gamma(\beta, \theta s x) dx.
\end{aligned}$$

It is clear that

$$K_1(z) = \frac{z^{\alpha-1}(1-z)^{\beta-1}}{B(\alpha, \beta)}. \quad (11)$$

By using the identity of Proposition A.3:

$$\int_0^\infty x^{a-1} \exp(-sx) \gamma(b, \theta x) dx = \frac{\theta^b \Gamma(a+b)}{b(s+\theta)^{a+b}} {}_2F_1\left(a+b, 1; b+1; \frac{\theta}{s+\theta}\right), \quad (12)$$

we have

$$K_2(z) = \frac{2\Gamma(2\alpha+\beta)}{\alpha\Gamma^2(\alpha)\Gamma(\beta)} \frac{z^{2\alpha-1}(1-z)^{\beta-1}}{(1+z)^{2\alpha+\beta}} {}_2F_1\left(1, 2\alpha+\beta; 1+\alpha; \frac{z}{1+z}\right) \quad (13)$$

and

$$K_3(z) = \frac{2\Gamma(\alpha+2\beta)}{\beta\Gamma(\alpha)\Gamma^2(\beta)} \frac{z^{\alpha-1}(1-z)^{2\beta-1}}{(2-z)^{\alpha+2\beta}} {}_2F_1\left(1, \alpha+2\beta; 1+\beta; \frac{1-z}{2-z}\right). \quad (14)$$

Furthermore, by using the identity of Proposition A.2:

$$\begin{aligned}
&\int_0^\infty x^{a-1} \exp(-sx) \gamma(b, \theta x) \gamma(c, \xi x) dx \\
&= \frac{\theta^b \xi^c \Gamma(a+b+c)}{bc(s+\theta+\xi)^{a+b+c}} F_2\left(a+b+c, 1, 1; b+1, c+1; \frac{\theta}{s+\theta+\xi}, \frac{\xi}{s+\theta+\xi}\right), \quad (15)
\end{aligned}$$

we obtain

$$K_4(z) = \frac{4^{1-\alpha-\beta} \Gamma(2\alpha+2\beta)}{\alpha\beta\Gamma^2(\alpha)\Gamma^2(\beta)} z^{2\alpha-1} (1-z)^{2\beta-1} F_2\left(2\alpha+2\beta, 1, 1; \alpha+1, \beta+1; \frac{z}{2}, \frac{1-z}{2}\right). \quad (16)$$

By replacing (11), (13), (14) and (16) in (9), we get (for $0 < z < 1$)

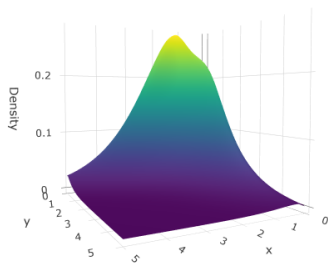
$$\begin{aligned}
f_{\frac{X}{X+Y}}(z) &= (1 + \rho) \frac{z^{\alpha-1}(1-z)^{\beta-1}}{B(\alpha, \beta)} \\
&\quad - \frac{2\rho\Gamma(2\alpha + \beta)}{\alpha\Gamma^2(\alpha)\Gamma(\beta)} \frac{z^{2\alpha-1}(1-z)^{\beta-1}}{(1+z)^{2\alpha+\beta}} {}_2F_1\left(1, 2\alpha + \beta; 1 + \alpha; \frac{z}{1+z}\right) \\
&\quad - \frac{2\rho\Gamma(\alpha + 2\beta)}{\beta\Gamma(\alpha)\Gamma^2(\beta)} \frac{z^{\alpha-1}(1-z)^{2\beta-1}}{(2-z)^{\alpha+2\beta}} {}_2F_1\left(1, \alpha + 2\beta; 1 + \beta; \frac{1-z}{2-z}\right) \\
&\quad + \frac{4^{1-\alpha-\beta}\rho\Gamma(2\alpha + 2\beta)}{\alpha\beta\Gamma^2(\alpha)\Gamma^2(\beta)} z^{2\alpha-1}(1-z)^{2\beta-1} F_2\left(2\alpha + 2\beta, 1, 1; \alpha + 1, \beta + 1; \frac{z}{2}, \frac{1-z}{2}\right) \\
&= f_Z(z; \boldsymbol{\theta}).
\end{aligned}$$

Therefore, we have proven that

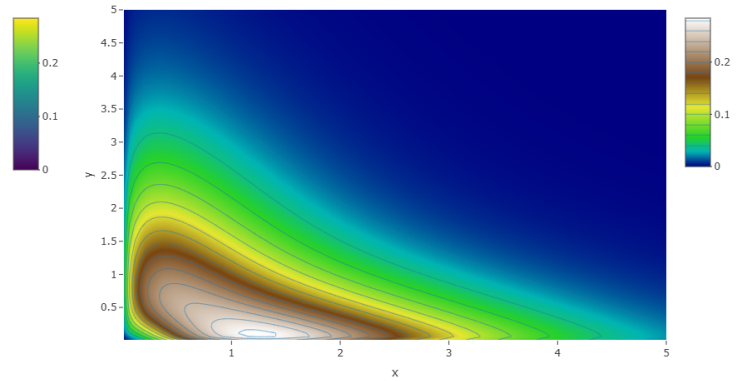
$$f_{\frac{X}{X+Y}}(z) = f_Z(z; \boldsymbol{\theta}), \quad 0 < z < 1. \quad (17)$$

In other words, the stochastic representation for Z given in (6) is valid.

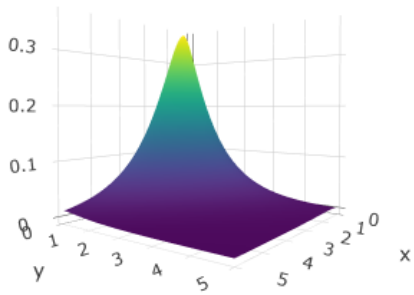
Figure 4 shows the joint PDF of Morgenstern's bivariate distribution with Gamma margins and contour lines of the joint density, for fixed $\alpha = 1.1$ and $\beta = 1.5$ and varying $\rho \in \{-0.99, 0, 0.75\}$. Note that when $\rho = -0.99$, a possible local maximum appears near the global maximum. This corresponds to the same parameter configuration that produced bimodality in one of the plots in Figure 3.



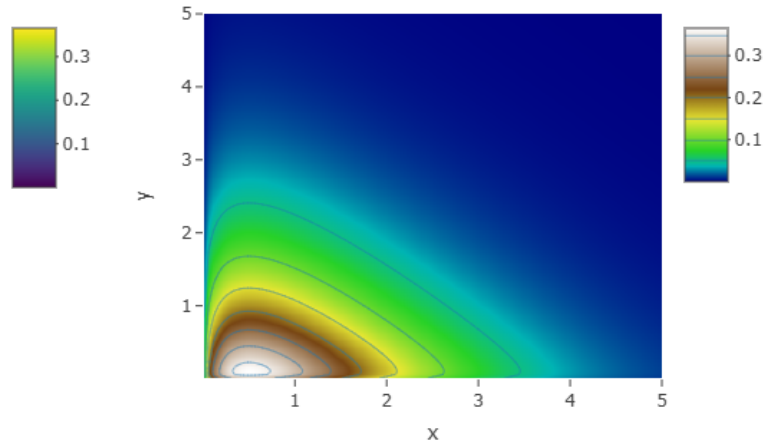
(a) $\rho = -0.99$



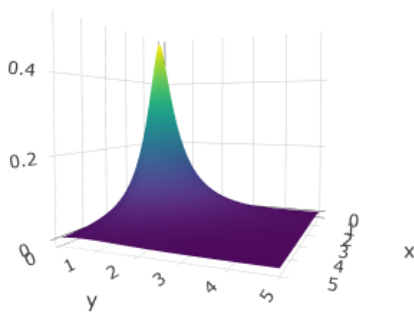
(b) $\rho = -0.99$



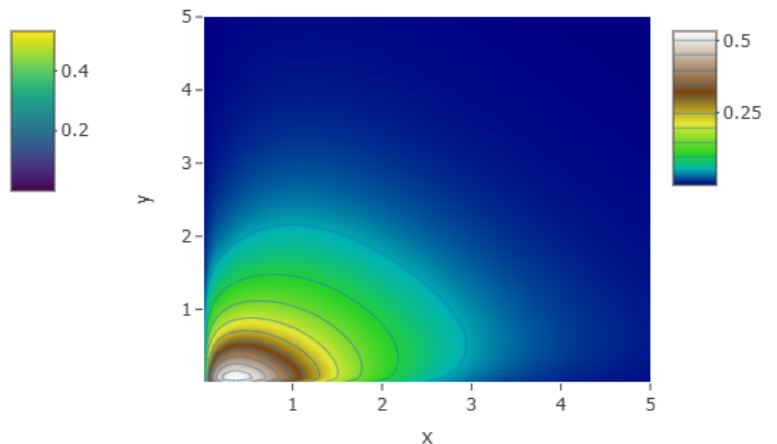
(c) $\rho = 0$



(d) $\rho = 0$



(e) $\rho = 0.75$



(f) $\rho = 0.75$

Figure 4: Joint PDF of Morgenstern's bivariate distribution with Gamma margins and contour lines of the joint density for $\rho = -0.99$ in (a) and (b), $\rho = 0$ in (c) and (d), and $\rho = 0.75$ in (e) and (f). $\alpha = 1.1$ and $\beta = 1.5$.

3.3 Other characterizations of EBB model

Let X and Y be two (absolutely) continuous positive random variables with CDFs F_X and F_Y , respectively. Based on F_X and F_Y and its respective PDFs f_X and f_Y , we define two new densities g_X and g_Y as follows:

$$g_X(x) = 2f_X(x)F_X(x), \quad g_Y(y) = 2f_Y(y)F_Y(y), \quad x, y > 0. \quad (18)$$

Proposition 3.1. The non-negative functions f_1, f_2, f_3 and f_4 defined as (for $s = 1/z - 1$ and $0 < z < 1$)

$$\begin{aligned} f_1(z) &\equiv (s+1)^2 \int_0^\infty x f_X(x) f_Y(sx) dx, \\ f_2(z) &\equiv (s+1)^2 \int_0^\infty x g_X(x) f_Y(sx) dx, \\ f_3(z) &\equiv (s+1)^2 \int_0^\infty x f_X(x) g_Y(sx) dx, \\ f_4(z) &\equiv (s+1)^2 \int_0^\infty x g_X(x) g_Y(sx) dx, \end{aligned} \quad (19)$$

are PDFs. In the above, g_X and g_Y are as in (18).

Proof. Let p and q be two arbitrary densities with positive support. In what follows, we prove that the function g defined as (for $s = 1/z - 1$ and $0 < z < 1$)

$$g(z) \equiv (s+1)^2 \int_0^\infty x p(x) q(sx) dx$$

is a PDF. Indeed, since

$$\int_0^1 g(z) dz = \int_0^\infty x p(x) \left[\int_0^1 \frac{1}{z^2} q\left(\left(\frac{1}{z} - 1\right)x\right) dz \right] dx,$$

taking the change of variable $y = (1/z - 1)x$, the right-hand integral is written as

$$= \int_0^\infty x p(x) \left[\frac{1}{x} \int_0^\infty q(y) dy \right] dx = 1,$$

where in the last equality, we have used the fact that p and q are PDFs.

Hence, taking (i) $p = f_X$ and $q = f_Y$, (ii) $p = g_X$ and $q = f_Y$, (iii) $p = f_X$ and $q = g_Y$, and (iv) $p = g_X$ and $q = g_Y$, it follows that f_1, f_2, f_3 and f_4 in (19) are PDFs. \square

Since $f_i(z) = K_i(z)$, $i = 1, 2, 3, 4$, where K_i is as in (10), from (9), we have (for $0 < z < 1$)

$$f_{\frac{X}{X+Y}}(z) = (1 + \rho) f_1(z) - \rho f_2(z) - \rho f_3(z) + \rho f_4(z). \quad (20)$$

If furthermore, $(X, Y)^\top$ follows a Morgenstern's bivariate distribution (with gamma margins), then, by (17) and (20), we have

$$f_Z(z; \boldsymbol{\theta}) = f_{\frac{X}{X+Y}}(z) = \sum_{i=1}^4 \pi_i f_i(z), \quad 0 < z < 1,$$

where $\pi_1 = 1 + \rho$, $\pi_2 = \pi_3 = -\rho$ and $\pi_4 = \rho$. In other words, if Z_i is a continuous positive random variable having PDF $f_i(z)$, $0 < z < 1$, $i = 1, 2, 3, 4$, where $X \sim \text{Gamma}(\alpha, \theta)$ and $Y \sim \text{Gamma}(\beta, \theta)$, then

$$Z \stackrel{d}{=} \frac{X}{X+Y} \stackrel{d}{=} \sum_{i=1}^4 \mathbb{1}_{\{B=i\}} Z_i, \quad (21)$$

where B is a discrete random variable independent of Z_1, Z_2, Z_3 and Z_4 , assuming values on the finite set $\{1, 2, 3, 4\}$ with probability mass function $\mathbb{P}(B = 1) = \pi_1$, $\mathbb{P}(B = 2) = \pi_2$, $\mathbb{P}(B = 3) = \pi_3$ and $\mathbb{P}(B = 4) = \pi_4$.

Proposition 3.2. Suppose that

- (a) X_1 and Y_1 are independent variables having densities $f_X(x)$ and $f_Y(x)$, respectively;
- (b) X_2 and Y_2 are independent variables having densities $g_X(x)$ and $f_Y(x)$, respectively;
- (c) X_3 and Y_3 are independent variables having densities $f_X(x)$ and $g_Y(x)$, respectively;
- (d) X_4 and Y_4 are independent variables having densities $g_X(x)$ and $g_Y(x)$, respectively.

If Z_i has PDF $f_i(z)$, $i = 1, 2, 3, 4$, given in (19), then

$$Z_i = \frac{X_i}{X_i + Y_i}, \quad i = 1, 2, 3, 4.$$

Proof. The proof follows by using the Jacobian method and then by determining the marginal with respect to Z_i of the random vector $(Z_i, U_i)^\top$, where $Z_i = X_i/(X_i + Y_i)$ and $U_i = Y_i$, $i = 1, 2, 3, 4$. \square

By combining (21) and Proposition 3.2, with $(X, Y)^\top$ following a Morgenstern's bivariate distribution (with gamma margins), we get

$$Z \stackrel{d}{=} \frac{X}{X+Y} \stackrel{d}{=} \sum_{i=1}^4 \mathbb{1}_{\{B=i\}} Z_i = \sum_{i=1}^4 \mathbb{1}_{\{B=i\}} \frac{X_i}{X_i + Y_i}, \quad (22)$$

where $B \in \{1, 2, 3, 4\}$ is a discrete random variable independent of Z_1, Z_2, Z_3 and Z_4 .

3.4 The cumulative distribution function

Using the stochastic representation of $Z \sim \text{EBB}(\boldsymbol{\theta})$, given in (6), by the Law of total expectation we have (for $s = 1/z - 1$ and $0 < z < 1$)

$$\begin{aligned} F_Z(z; \boldsymbol{\theta}) &= \mathbb{P}\left(\frac{X}{X+Y} \leq z\right) = \mathbb{P}(sX \leq Y) = 1 - \mathbb{P}(Y \leq sX) \\ &= 1 - \int_0^\infty \mathbb{P}(Y \leq sX | X = x) f_X(x) dx \\ &= 1 - \int_0^\infty \int_0^{sx} f_{X,Y}(x, y) dy dx. \end{aligned} \quad (23)$$

Since $(X, Y)^\top$ has Morgenstern's bivariate distribution (7)-(8) (with gamma margins) (see Subsection 3.2), the above identities are briefly written as

$$F_Z(z; \boldsymbol{\theta}) = 1 - \int_0^{\infty} f_X(x) \left\{ F_Y(sx) + \rho [2F_X(x) - 1] \left[\int_0^{sx} 2f_Y(y)F_Y(y)dy - F_Y(sx) \right] \right\} dx. \quad (24)$$

As $Y \sim \text{Gamma}(\beta, \theta)$, from Proposition A.1 in Appendix, we obtain

$$\int_0^{sx} 2f_Y(y)F_Y(y)dy = \frac{2\theta^\beta}{\Gamma^2(\beta)} \int_0^{sx} y^{\beta-1} \exp(-\theta y) \gamma(\beta, \theta y) dy = 2 \frac{\gamma(\beta, \theta sx)}{\Gamma(\beta)} - 1. \quad (25)$$

As $X \sim \text{Gamma}(\alpha, \theta)$ and $Y \sim \text{Gamma}(\beta, \theta)$, by using (25), $F_Z(z; \boldsymbol{\theta})$ in (24) is written as

$$\begin{aligned} F_Z(z; \boldsymbol{\theta}) &= 1 - \frac{\theta^\alpha}{\Gamma(\alpha)} \int_0^{\infty} x^{\alpha-1} \exp(-\theta x) \left[\frac{\gamma(\beta, \theta sx)}{\Gamma(\beta)} + \rho \left\{ 2 \frac{\gamma(\alpha, \theta x)}{\Gamma(\alpha)} - 1 \right\} \left\{ \frac{\gamma(\beta, \theta sx)}{\Gamma(\beta)} - 1 \right\} \right] dx \\ &= 1 + \frac{(\rho - 1)\theta^\alpha}{\Gamma(\alpha)\Gamma(\beta)} \int_0^{\infty} x^{\alpha-1} \exp(-\theta x) \gamma(\beta, \theta sx) dx \\ &\quad - \frac{2\rho\theta^\alpha}{\Gamma^2(\alpha)\Gamma(\beta)} \int_0^{\infty} x^{\alpha-1} \exp(-\theta x) \gamma(\alpha, \theta x) \gamma(\beta, \theta sx) dx \\ &\quad + \frac{2\rho\theta^\alpha}{\Gamma^2(\alpha)} \int_0^{\infty} x^{\alpha-1} \exp(-\theta x) \gamma(\alpha, \theta x) dx - \frac{\rho\theta^\alpha}{\Gamma(\alpha)} \int_0^{\infty} x^{\alpha-1} \exp(-\theta x) dx. \end{aligned}$$

By using the identities in (12) and (15), and Proposition A.1 with $x \rightarrow \infty$ and α instead β (see Appendix), we have (for $0 < z < 1$)

$$\begin{aligned} F_Z(z; \boldsymbol{\theta}) &= 1 + \frac{\rho - 1}{\beta B(\alpha, \beta)} z^\alpha (1 - z)^\beta {}_2F_1(1, \alpha + \beta; 1 + \beta; 1 - z) \\ &\quad - \frac{2\rho\Gamma(2\alpha + \beta)}{\alpha\beta\Gamma^2(\alpha)\Gamma(\beta)} \frac{z^{2\alpha}(1 - z)^\beta}{(1 + z)^{2\alpha + \beta}} F_2\left(2\alpha + \beta, 1, 1; \alpha + 1, \beta + 1; \frac{z}{1 + z}, \frac{1 - z}{1 + z}\right). \end{aligned}$$

By using the well-known identity

$$B_x(a, b) = \frac{x^a(1 - x)^b}{a} {}_2F_1(1, a + b; 1 + a; x),$$

where $B_x(a, b) = \int_0^x t^{a-1}(1 - t)^{b-1} dt$ is the incomplete beta function, we write $F_Z(z)$ as follows (for $0 < z < 1$)

$$\begin{aligned} F_Z(z; \boldsymbol{\theta}) &= 1 + (\rho - 1)I_{1-z}(\beta, \alpha) \\ &\quad - \frac{2\rho\Gamma(2\alpha + \beta)}{\alpha\beta\Gamma^2(\alpha)\Gamma(\beta)} \frac{z^{2\alpha}(1 - z)^\beta}{(1 + z)^{2\alpha + \beta}} F_2\left(2\alpha + \beta, 1, 1; \alpha + 1, \beta + 1; \frac{z}{1 + z}, \frac{1 - z}{1 + z}\right), \quad (26) \end{aligned}$$

where $I_z(a, b) = B_z(a, b)/B(a, b)$ is the regularized incomplete beta function.

Remark 3.3. When $\rho = 0$, by using the well-known identity $I_z(\alpha, \beta) = 1 - I_{1-z}(\beta, \alpha)$, we have (for $0 < z < 1$)

$$F_Z(z; \boldsymbol{\theta}) = I_z(\alpha, \beta),$$

which is a very well-known result in the literature.

3.5 Moment-generating function and moments

Given that $Z \sim \text{EBB}(\theta)$ has unitary support, its moment-generating function (MGF), $M_Z(t)$, and raw moments, μ_n , $n \in \mathbb{N}$, exist and are finite, particularly within an open interval encompassing zero. Then $M_Z(t)$ may be expanded in a power series about 0 in the following form

$$M_Z(t) = 1 + \sum_{n=1}^{\infty} \frac{\mu_n}{n!} t^n.$$

In what follows we derive a closed-form expression for μ_n . Indeed, by using the well-known formula for moments of positive order $\mathbb{E}(X^p) = p \int_0^{\infty} x^{p-1} \mathbb{P}(X > x) dx$ of positive random variables, we have

$$\mu_n = n \int_0^1 z^{n-1} [1 - F_Z(z; \theta)] dz,$$

where $F_Z(z; \theta)$ is as in (26). So, from (26),

$$\begin{aligned} \mu_n &= n(1 - \rho) \int_0^1 z^{n-1} I_{1-z}(\beta, \alpha) dz \\ &+ \frac{2n\rho\Gamma(2\alpha + \beta)}{\alpha\beta\Gamma^2(\alpha)\Gamma(\beta)} \int_0^1 \frac{z^{n+2\alpha-1}(1-z)^\beta}{(1+z)^{2\alpha+\beta}} F_2\left(2\alpha + \beta, 1, 1; \alpha + 1, \beta + 1; \frac{z}{1+z}, \frac{1-z}{1+z}\right) dz. \end{aligned} \quad (27)$$

For the particular scenario where $\alpha = \beta$, we obtain $\mu_1 = 1/2$ (see Subsection 3.1). Due to the integral's complexity in (27), numerical methods are requisite for its computation.

4 Estimation

The log-likelihood function for $\theta = (\alpha, \beta, \rho)^\top$ based on a sample of n independent observations is given by

$$\begin{aligned} \ell(\theta) &= \sum_{i=1}^n \log \left[(1 + \rho) \frac{z_i^{\alpha-1} (1 - z_i)^{\beta-1}}{\text{B}(\alpha, \beta)} \right. \\ &- \frac{2\rho\Gamma(2\alpha + \beta)}{\alpha\Gamma^2(\alpha)\Gamma(\beta)} \frac{z_i^{2\alpha-1} (1 - z_i)^{\beta-1}}{(1 + z_i)^{2\alpha+\beta}} {}_2F_1\left(1, 2\alpha + \beta; 1 + \alpha; \frac{z_i}{1 + z_i}\right) \\ &- \frac{2\rho\Gamma(\alpha + 2\beta)}{\beta\Gamma(\alpha)\Gamma^2(\beta)} \frac{z_i^{\alpha-1} (1 - z_i)^{2\beta-1}}{(2 - z_i)^{\alpha+2\beta}} {}_2F_1\left(1, \alpha + 2\beta; 1 + \beta; \frac{1 - z_i}{2 - z_i}\right) \\ &+ \frac{4^{1-\alpha-\beta}\rho\Gamma(2\alpha + 2\beta)}{\alpha\beta\Gamma^2(\alpha)\Gamma^2(\beta)} \frac{z_i^{2\alpha-1} (1 - z_i)^{2\beta-1}}{z_i^{2\alpha-1} (1 - z_i)^{2\beta-1}} \\ &\left. \times F_2\left(2\alpha + 2\beta, 1, 1; \alpha + 1, \beta + 1; \frac{z_i}{2}, \frac{1 - z_i}{2}\right) \right]. \end{aligned} \quad (28)$$

The maximum likelihood estimator (MLE) $\hat{\theta} = (\hat{\alpha}, \hat{\beta}, \hat{\rho})^\top$ of $\theta = (\alpha, \beta, \rho)^\top$ is obtained by the maximization of the log-likelihood function (28). However, it is not possible to derive an analytical solution

for the MLE $\widehat{\boldsymbol{\theta}}$; therefore, we must require a numerical solution using some optimization algorithm such as Newton–Raphson and quasi-Newton. But, computations of likelihood $\ell(\boldsymbol{\theta})$ can be extremely costly due to the dependence of PDF (2) and CDF (26) on special functions such as the Gauss hypergeometric ${}_2F_1$ and Appell F_2 . Moreover, optimization methods may not converge properly.

Thus, our strategy is as follows: given a random sample from (X, Y) , we first fit the margins as $\text{Gamma}(\alpha, 1)$ and $\text{Gamma}(\beta, 1)$, and then estimate the dependence parameter ρ in a second stage. Thus, comparing X and Y through $Z = X/(X + Y)$, we obtain a natural estimator for the parameters of Z . Naturally, we can first use the estimates from the $\text{Beta}(\alpha, \beta)$ model and then estimate ρ in a second stage, thus improving the initial Beta fit. The algorithm is summarized in the two steps below:

1. Given a random sample $\mathbf{Z} = (Z_1, \dots, Z_n) \in [0, 1]^n$, use the ML estimators of the Beta model to obtain $(\hat{\alpha}, \hat{\beta}) = (\hat{\alpha}(\mathbf{Z}), \hat{\beta}(\mathbf{Z}))$;
2. estimate ρ using an appropriate optimization algorithm.

These steps are effective in scenarios where the Beta model provides a good initial fit to the data.

Taking into account the second stage, the estimation of ρ ,

- if Z is observed directly in $[0, 1]$, we can use

$$\widehat{\rho} \in \arg \max_{\rho \in [0, 1]} \ell(\rho), \quad (29)$$

where $\ell(\rho) := \ell(\boldsymbol{\theta}) |_{(\alpha, \beta) = (\hat{\alpha}, \hat{\beta})}$;

- if $Z = \frac{X}{X+Y}$, then, using Theorem 2 in Lai (1978), we obtain the estimator

$$\widehat{\rho} = \frac{\widehat{\text{corr}}(X, Y) \widehat{\sigma}_x \widehat{\sigma}_y}{\widehat{\beta}_x \widehat{\beta}_y}, \quad (30)$$

where $\sigma_x = \text{Var } X$, $\sigma_y = \text{Var } Y$, $\beta_x = \int_0^\infty G(x; \alpha, 1) [1 - G(x; \alpha, 1)] dx$, and

$$\beta_y = \int_0^\infty G(x; \beta, 1) [1 - G(x; \beta, 1)] dx,$$

in which $G(\cdot; \theta, 1)$ denotes the CDF of a Gamma model with shape θ and scale 1.

5 Simulation study

5.1 Random sample generator

Define the bivariate function $C : [0, 1] \times [0, 1] \rightarrow [0, 1]$ as

$$C(u_1, u_2) = u_1 u_2 [1 + \rho(1 - u_1)(1 - u_2)], \quad (u_1, u_2) \in [0, 1] \times [0, 1] \text{ and } -1 \leq \rho \leq 1. \quad (31)$$

Note that the bivariate distribution function $F_{X,Y}(x, y)$ given in (7) is a composition of $C(\cdot, \cdot)$ with margins Gamma CDFs $(F_X(x), F_Y(y))$, where $X \sim \text{Gamma}(\alpha, \theta)$ and $Y \sim \text{Gamma}(\beta, \theta)$. That is,

$$F_{X,Y}(x, y) = C(F_X(x), F_Y(y)), \quad x, y > 0.$$

Aiming to simulate a random sample Z_1, \dots, Z_n from the extended Beta PDF (2), we use the Algorithm 1, which simulates $Z = \frac{X}{X+Y} \sim f_Z(\cdot; \boldsymbol{\theta})$ based on a simulation of $(X, Y) \sim F_{X,Y}$. For a further discussion on this algorithm, we refer the reader to Mai and Scherer (2017).

Algorithm 1 Computational sampling of the extended Beta distribution

Input: $\theta = (\alpha, \beta, \rho)^\top \in (0, \infty)^2 \times [-1, 1]$.

Output: $Z \sim f_Z(\cdot; \theta)$.

- 1: Simulate $U_2 \sim U[0, 1]$.
- 2: Compute the partial derivative

$$F_{U_1|U_2}(u_1) := \left. \frac{\partial}{\partial u_2} C(u_1, u_2) \right|_{u_2=U_2} = u_1 [1 + \rho(1 - u_1)(1 - 2u_2)], \quad u_1 \in [0, 1].$$

- 3: Compute the generalized inverse $F_{U_1|U_2}^{-1}$ numerically:

$$F_{U_1|U_2}^{-1}(v) := \inf \{u_1 > 0; F_{U_1|U_2}(u_1) \geq v\}, \quad v \in (0, 1),$$

- 4: Get a sample $V \sim U[0, 1]$, independent of U_2 .
- 5: Define $U_1 := F_{U_1|U_2}^{-1}(V)$ and take (U_1, U_2) as the random vector of the copula C .
- 6: Compute $(X, Y) \sim F_{X,Y}$ as

$$(X, Y) = (F_X^{-1}(U_1), F_Y^{-1}(U_2)),$$

where $F_{X,Y}$ is given in (7) and F_X and F_Y denote the CDFs of Gamma models as described in Subsection 3.4.

- 7: **Return** $Z = \frac{X}{X+Y}$.
-

5.2 R implementation and required packages

For this study, all implementations were performed in R software (R Core Team, 2025).

We implement the Appell function F_2 in R using the double series (3). The convergence region of (3) is sufficient to implement PDF (2) and CDF (26) of the EBB model. For other function implementations, a wider range may be required. In such cases, numerical integral representations can be employed. Some additional formulas for the Appell function F_2 can be found in Brychkov and Saad (2014) and Ananthanarayan et al. (2023). The generalized hypergeometric function is computed using `hyperg_2F1` from the `gsl` package. Thus, the probability density function (PDF) (2) can be implemented in R.

Referring to the Algorithm 1, the numerical inverse is required. We achieve this by the function `uniroot`.

A gradient-based method can be applied to optimize the log-likelihood function. The gradient of the objective function is obtained using the function `grad` in the package `numDeriv`.

Remark 5.1. Another simulation algorithm could be proposed by directly inverting the CDF (26) and applying it to a standard uniform random variable.

5.3 Simulation results

To evaluate the performance of the ML estimator $\hat{\theta}$, we fix several values of the parameters $\theta = (\alpha, \beta, \rho)^\top$, and then generate $N = 1,000$ Monte-Carlo samples with sample size $n \in \{30, 100, 300, 1000\}$, of the random variable $Z \sim EBB(\alpha, \beta, \rho)$. We analyze estimates $\hat{\theta}$ through relative bias (RB), and root mean squared error (RMSE).

We use the gradient descent algorithm to achieve the minimum of the minus log-likelihood function (cf. [Shalev-Shwartz and Ben-David, 2014](#)) to obtain the ML estimates for the EBB distribution. The gradient of the objective function can be obtained numerically, as described in Subsection 5.2.

For the simulation, the following procedure was carried out:

Algorithm 2 Assessing ML estimates via Monte Carlo simulation

Input: $\theta = (\alpha, \beta, \rho)^\top \in (0, \infty)^2 \times [-1, 1]$, n (sample size), N (number of Monte Carlo simulations)

Output: RB and RMSE of ML estimates.

- 1: **for** $j = 1$ to N **do**
- 2: Simulate a Monte-Carlo sample $\mathbf{Z}^{(j)} = (Z_1^{(j)}, \dots, Z_n^{(j)})$ via Algorithm 1.
- 3: Compute $\hat{\theta}^{(j)} = \hat{\theta}^{(j)}(\mathbf{Z}^{(j)})$.
- 4: **end for**
- 5: Compute the RB and RMSE as follows:

$$RB(\hat{\theta}_k) = \frac{1}{N} \sum_{j=1}^N \frac{\hat{\theta}_k^{(j)} - \theta_k}{\theta_k}, \quad k = 1, 2, 3, \text{ and } \theta_1 = \alpha, \theta_2 = \beta, \theta_3 = \rho,$$

and

$$RMSE(\hat{\theta}_k) = \frac{1}{N} \sum_{j=1}^N \left(\hat{\theta}_k^{(j)} - \theta_k \right)^2.$$

- 6: **Return** $RB(\hat{\theta}_k)$ and $RMSE(\hat{\theta}_k)$ for $k = 1, 2, 3$, and $\theta_1 = \alpha, \theta_2 = \beta, \theta_3 = \rho$.
-

The simulation results are presented in Figures 5 and 6. The ML estimator shows good behavior with minimal RB and low RMSE. Furthermore, it is clear that increasing the sample size n leads RB and RMSE to approach zero. This demonstrates the precision of the ML estimator for the UF distribution, even with small sample sizes. Additionally, we observe that the RMSE of ρ estimates is less affected by variations in sample size. In general, for $n \geq 100$, the RB is below 0.10 and converges to zero as n increases. Although relatively low (in absolute values), the relative bias of ρ exhibited a different sign compared to the estimates of the parameters α and β .

Regarding the RMSE, large values were observed in some cases for small sample sizes. However, the value decreased when larger samples were taken ($n \in \{300, 1000\}$). The RMSE of the β estimates was high (≥ 0.5) when $n = 30$, in both cases $\rho = -0.5$ and $\rho = 0.5$. When $n = 100$, the values decreased to 0.20, stabilizing below 0.10 only for $n \geq 300$.

In Figure 7, we fixed $\theta^\top = (2, 3, 0.5)$ and plotted the histogram of Monte Carlo simulation results of estimates. When $n = 30$ (top), the estimates of the three parameters were right-skewed. We can see that as n increases, the figures become symmetric, showing the good asymptotic behavior of the estimates. The same behavior occurs with the other parameters studied.

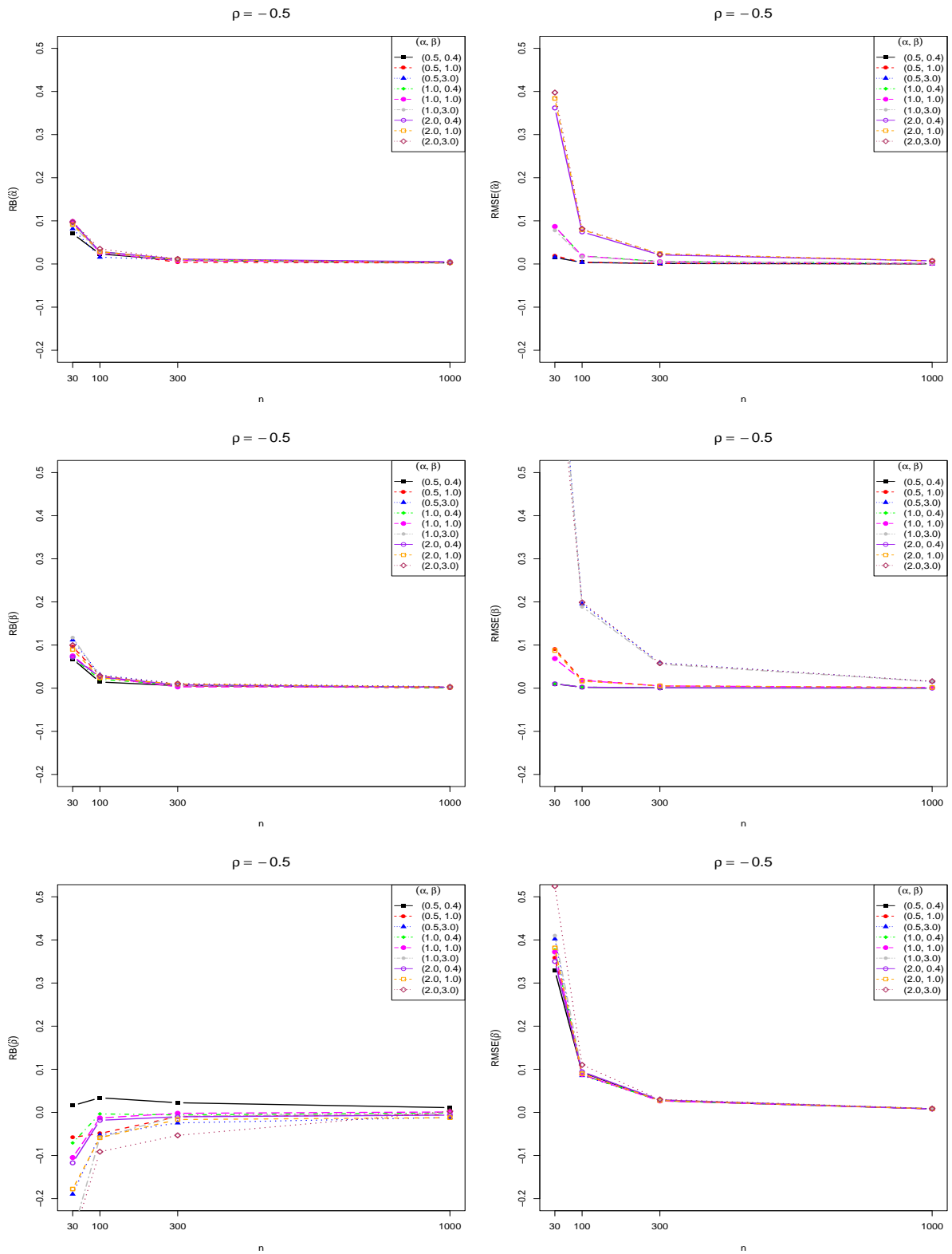


Figure 5: RB (left) and RMSE (right) for the ML estimates of α (top), β (middle), and ρ (bottom), with varying (α, β) and fixing negative $\rho = -0.5$.

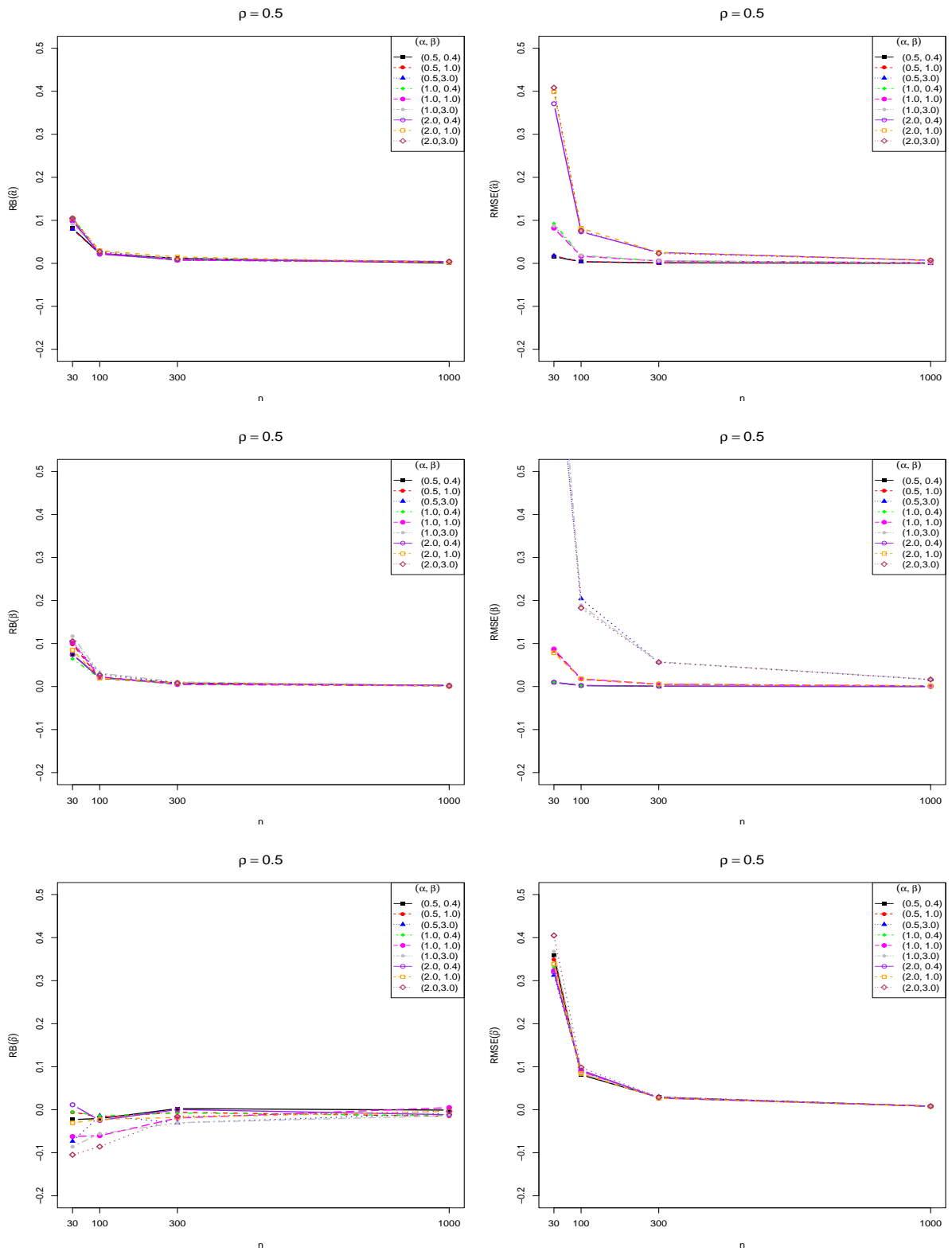


Figure 6: RB (left) and RMSE (right) for the ML estimates of α (top), β (middle), and ρ (bottom), with varying (α, β) and fixing positive $\rho = 0.5$.

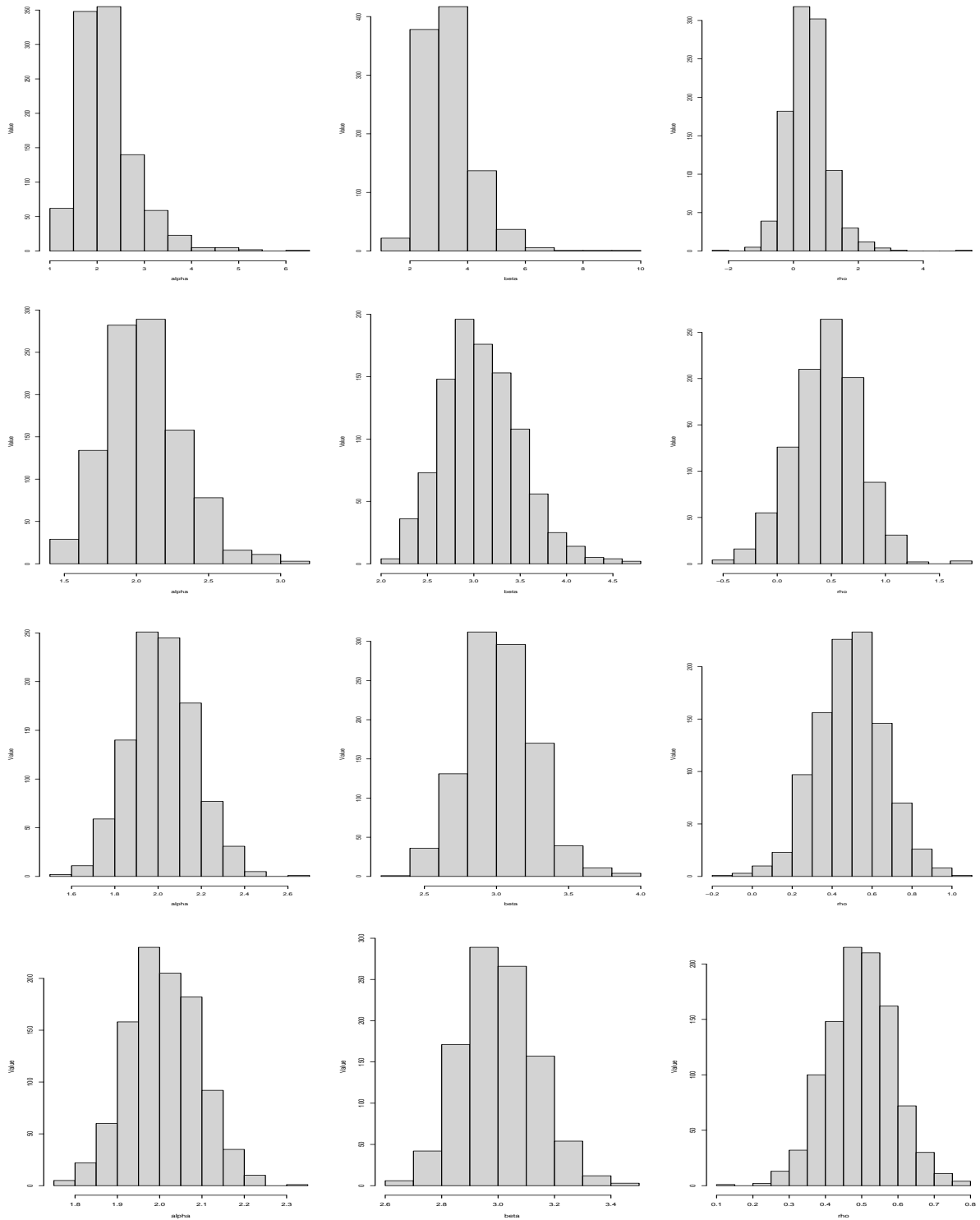


Figure 7: Histograms of Monte Carlo results for the ML estimates of α (left), β (middle), and ρ (right), with increasing sample size $n = 30$ (top), 100, 300, and 1000 (bottom).

6 Real-world data analysis

In this section, we present an application of the proposed model to real data for illustrative purposes. To ensure replicability of our results and provide support for future users of the EBB model, all R codes are publicly available at https://github.com/FSQuintino/extended_beta_model.git (accessed on 07 Jan 2026). A comparison with the well-known Beta and Kumaraswamy models is presented. For simplicity of notation, we set the parameters as α and β for all competing distributions. That means, the Beta and Kumaraswamy models have PDFs, respectively, given by

$$f_B(w; \alpha, \beta) = \frac{\Gamma(\alpha + \beta)}{\Gamma(\alpha)\Gamma(\beta)} w^{\alpha-1} (1 - w)^{\beta-1}, \quad 0 < w < 1, \quad (32)$$

and

$$f_K(w; \alpha, \beta) = \alpha\beta w^{\alpha-1} (1 - w^\alpha)^{\beta-1}, \quad 0 < w < 1.$$

The ML estimates for the above models were obtained using the `goodness.fit` function from the `AdequacyModel` package in R software.

6.1 Household financial fragility dataset

The dataset comes from the Bank of Italy’s Survey on Household Income and Wealth from the year 2008. We utilized data from the RFAM08 data set (with income as the Y variable) and the RISFAM08 data set (with expenditures as the C variable), as outlined in the Survey on Household Income and Wealth 2008 data description file. We excluded any data entries where income or consumption was negative or unavailable. The data were recently reported in [Vila and Quintino \(2026\)](#) and the references therein, and are available at https://www.bancaditalia.it/statistiche/tematiche/indagini-famiglie-impres/bilanci-famiglie/documentazione/ricerca/ricerca.html?min_anno_publicazione=2008&max_anno_publicazione=2008 (accessed on 20 November 2025). In this study, we analyze household financial fragility by constructing a new variable $Z = Y/(X + Y)$ based on (1), where X and Y represent expenditures and income. Values of $Z < 1/2$ indicate that the family ended the year with more expenditures than income. If $Z > 1/2$, the opposite is true. The case $Z = 1/2$ means expenditures and income are equal.

In Table 1, we present the following descriptive statistics: the sample size (n); the minimum value observed in the dataset (Min.); the first quartile value (1st Qu.); the median value (Median); the average value (Mean); the third quartile value (3rd Qu.); the maximum value observed (Max.); the standard deviation (Sd.); the coefficient of symmetry (CS); the coefficient of kurtosis (CK).

Table 1: Descriptive statistics for the household financial fragility dataset.

n	Min.	1st Qu.	Median	Mean	3rd Qu.	Max.	Sd	CS	CK
7957	0.00	0.51	0.55	0.56	0.61	0.94	0.09	-0.42	3.34

As pointed out in Subsection 3.2, the EB model arises from a ratio, where the random vector $(X, Y)^\top$ follows the Morgenstern bivariate distribution with gamma margins. Figure 8 shows the gamma fits of the marginal distributions of expenditures and income. These findings offer more support for the EB model’s good fit to the derived Z unitary data.

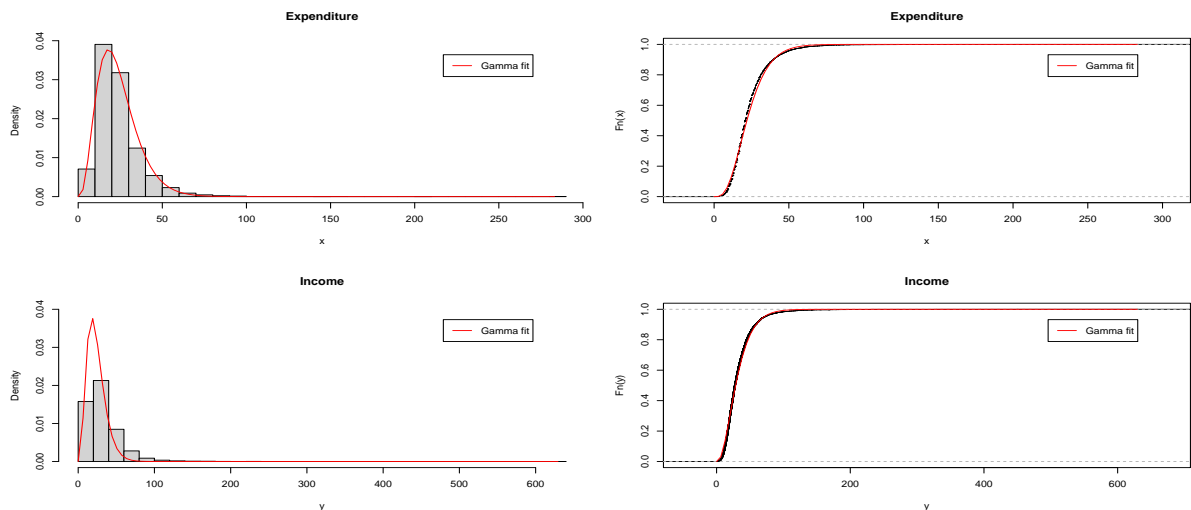


Figure 8: Gamma fits to marginal distributions of expenditures and income.

To estimate the EBB parameters for dataset Z, we applied (30). Due to the scale of the consumption-income data (X, Y) , we consider the equivalent form

$$Z = \frac{Y/10^3}{Y/10^3 + X/10^3}.$$

This adjustment is required to achieve numerical convergence in the estimation procedures. The choice of 10^3 is based on trials with 10^k . Varying k can either improve or worsen the estimation results, and in some cases may even render them numerically intractable. Table 2 gives the estimates, the Akaike information criterion (AIC) and Bayesian information criterion (BIC) for the fitted models. Since the values of the AIC and BIC are smaller for the EBB model compared with those values of the other model, this new model seems to be a competitive model for these data.

Table 2: Parameter estimates and model selection (AIC and BIC) for the household financial fragility dataset.

Model	$\hat{\alpha}$	$\hat{\beta}$	$\hat{\rho}$	$\ell(\hat{\theta})$	AIC	BIC
Beta	16.10	12.84		7832.86	-15661.72	-15647.76
Kumaraswamy	6.46	28.86		7795.81	-15587.63	-15573.66
EBB	16.10	12.84	0.78	7922.92	-15839.84	-15818.90

Plots of the PDF and CDF of the beta, kumaraswamy and EBB fitted models to these data are displayed in Figure 9. They indicate that the BSG distribution is superior to the other distributions in terms of model fitting. Additionally, it is evident that the kumaraswamy distribution presents the worst fit to the current data and then the proposed models outperform this distribution.

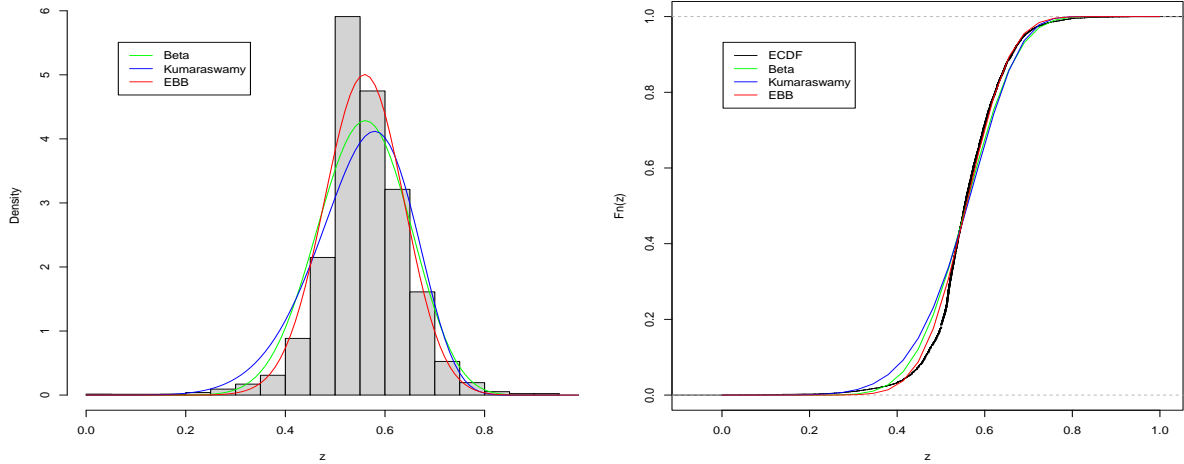


Figure 9: Histogram (left) and empirical CDF (right) compared with Beta, Kumaraswamy, and EBB models for the household financial fragility dataset.

To test the null hypothesis $H_0 : \rho = 0$ (H_0 : beta model) against the alternative hypothesis $H_1 : \rho \neq 0$ (H_1 : EBB model), we use the LR statistic the value of which is 180.12 (p-value < 0.01). Thus, using any usual significance level, we reject the null hypothesis in favor of the EBB model, i.e., this model is significantly better than the beta model for explaining the current data.

7 Concluding remarks

In this paper, we introduced the EBB distribution, a new unit-supported model obtained from the ratio of two correlated Gamma random variables following a Morgenstern-type dependence structure. The additional dependence parameter extends the classical Beta distribution while preserving interpretability. As shown throughout the paper, this extra flexibility allows the EBB family to accommodate a wide range of shapes, including symmetry, U- and J-shapes, and bimodality, which are often observed in applied problems but poorly captured by traditional unit models. Closed-form expressions were obtained for the probability density and cumulative distribution functions and moments, relying on tools from special-function theory. Estimation was addressed using likelihood-based and alternative methods, and a Monte Carlo study highlighted both the finite-sample behavior of the estimators and the computational challenges that may arise. Applications to real datasets demonstrated that the EBB distribution can provide improved fits compared to competing models, despite requiring only one additional parameter. Several directions remain open. Extensions to regression frameworks for responses to $(0, 1)$, Bayesian inference with informative priors, and multivariate generalizations are natural avenues for future research. Another promising line involves studying robustness properties and developing faster numerical strategies for likelihood maximization in large samples. In general, the EBB model adds a versatile and analytically tractable option to the family of unit distributions, with potential for broad application in economics, reliability, hydrology, and related fields.

Acknowledgements The research was supported in part by CNPq and CAPES grants from the Brazilian government.

Disclosure statement There are no conflicts of interest to disclose.

References

- Ahuja, J. C. (1969). On certain properties of the generalized Gompertz distribution. *Sankhyā*, B31:541–544.
- Ananthanarayan, B., Bera, S., Friot, S., Marichev, O., and Pathak, T. (2023). On the evaluation of the Appell F_2 double hypergeometric function. *Computer Physics Communications*, 284:108589.
- Appell, P. (1925). *Sur les fonctions hypergéométriques de plusieurs variables*, volume III of *Mémoires des Sciences Mathématiques de l'Académie des Sciences de Paris*. Gauthier-Villars, Paris.
- Brychkov, Y. A. and Saad, N. (2014). On some formulas for the Appell function $F_2(a, b, b'; c, c'; w; z)$. *Integral Transforms and Special Functions*, 25(2):111–123.
- D'Aurizio, J. (2016). Integrating the lower incomplete gamma $\int_0^\infty x^{a-1} e^{-sx} \gamma(b, x) dx$. <https://math.stackexchange.com/q/1825107>. Accessed: 2025-04-05.
- Kibble, W. F. (1941). A two-variate gamma type distribution. *Sankhyā*, 5:137–150.
- Lai, C. (1978). Morgenstern's bivariate distribution and its application to point processes. *Journal of Mathematical Analysis and Applications*, 65(2):247–256.
- Mai, J. and Scherer, M. (2017). *Simulating Copulas: Stochastic Models, Sampling Algorithms, and Applications*, volume 6 of *Series in Quantitative Finance 6*. World Scientific Publishing Company, 2nd edition.
- Malik, H. J. (1967). Exact distribution of the quotient of independent generalized gamma variables. *Canadian Mathematical Bulletin*, 10:463–465.
- Mathai, A., Saxena, R., and Haubold, H. (2010). *The H-function: Theory and Applications*. Springer Science & Business Media.
- Nadarajah, S. and Kotz, S. (2006). Bivariate gamma distributions, sums and ratios. *Bulletin of the Brazilian Mathematical Society*, 37:241–274.
- R Core Team (2025). *R: A Language and Environment for Statistical Computing*. R Foundation for Statistical Computing, Vienna, Austria.
- Shalev-Shwartz, S. and Ben-David, S. (2014). *Understanding machine learning: From theory to algorithms*. Cambridge university press.
- Vila, R., Alfaia, L., Menezes, A. F., Çankaya, M. N., and Bourguignon, M. (2024a). A model for bimodal rates and proportions. *Journal of Applied Statistics*, 51(4):664–681.

Vila, R., Balakrishnan, N., Saulo, H., and Zörnig, P. (2024b). Unit-log-symmetric models: characterization, statistical properties and their applications to analyzing an internet access data. *Quality & Quantity*, 58:4779–4806.

Vila, R. and Quintino, F. (2026). A novel unit-asymmetric distribution based on correlated Fréchet random variables. *Quality & Quantity*, 60:1443–1471.

Vila, R., Saulo, H., Quintino, F., and Zörnig, P. (2025). A new unit-bimodal distribution based on correlated birnbaum-saunders random variables. *Comp. Appl. Math.*, 44:83.

Appendix A Some additional results

The purpose of this section is to present and show some new technical results used throughout the work.

Proposition A.1. The following identity is valid (for $x > 0$)

$$\int_0^x y^{\beta-1} \exp(-\theta y) \gamma(\beta, \theta y) dy = \frac{\Gamma(\beta)}{\theta^\beta} \left[\gamma(\beta, \theta x) - \frac{\Gamma(\beta)}{2} \right],$$

where $\beta > 0$ and $\theta > 0$.

Proof. By using the definition of the lower incomplete gamma function:

$$\gamma(s, x) = \int_0^x t^{s-1} \exp(-t) dt, \quad (33)$$

we have

$$\int_0^x y^{\beta-1} \exp(-\theta y) \gamma(\beta, \theta y) dy = \int_0^x y^{\beta-1} \exp(-\theta y) \left[\int_0^{\theta y} t^{\beta-1} \exp(-t) dt \right] dy.$$

Interchanging the order of integration, the above integral is

$$\begin{aligned} &= \int_0^\infty t^{\beta-1} \exp(-t) \left[\int_{t/\theta}^x y^{\beta-1} \exp(-\theta y) dy \right] dt \\ &= \frac{1}{\theta^\beta} \int_0^\infty t^{\beta-1} \exp(-t) [\gamma(\beta, \theta x) - \gamma(\beta, t)] dt = \frac{\gamma(\beta, \theta x) \Gamma(\beta)}{\theta^\beta} - \frac{1}{\theta^\beta} \int_0^\infty t^{\beta-1} \exp(-t) \gamma(\beta, t) dt. \end{aligned}$$

In short, we have proven that

$$\int_0^x y^{\beta-1} \exp(-\theta y) \gamma(\beta, \theta y) dy = \frac{\gamma(\beta, \theta x) \Gamma(\beta)}{\theta^\beta} - \frac{1}{\theta^\beta} \int_0^\infty t^{\beta-1} \exp(-t) \gamma(\beta, t) dt. \quad (34)$$

Letting $x \rightarrow \infty$ and $\theta = 1$ in (34), we get

$$\int_0^\infty t^{\beta-1} \exp(-t) \gamma(\beta, t) dt = \frac{\Gamma^2(\beta)}{2}, \quad (35)$$

where we have used the fact that $\lim_{x \rightarrow \infty} \gamma(\beta, x) = \Gamma(\beta)$. Replacing (35) in (34), we have

$$\int_0^x y^{\beta-1} \exp(-\theta y) \gamma(\beta, \theta y) dy = \frac{\gamma(\beta, \theta x) \Gamma(\beta)}{\theta^\beta} - \frac{\Gamma^2(\beta)}{2\theta^\beta}.$$

This concludes the proof. □

The proof of the following result follows the same ideas set out in reference [D'Aurizio \(2016\)](#).

Proposition A.2. The following identity is valid

$$\begin{aligned} \int_0^\infty x^{a-1} \exp(-sx) \gamma(b, \theta x) \gamma(c, \xi x) dx \\ = \frac{\theta^b \xi^c \Gamma(a+b+c)}{bc(s+\theta+\xi)^{a+b+c}} F_2 \left(a+b+c, 1, 1; b+1, c+1; \frac{\theta}{s+\theta+\xi}, \frac{\xi}{s+\theta+\xi} \right), \end{aligned}$$

where $a > 0$, $s > 0$, $\theta > 0$, $\xi > 0$, $b > 0$ and $c > 0$.

Proof. By using the definition (33) of lower incomplete gamma function, we have

$$\gamma(b, \theta x) = \int_0^{\theta x} y^{b-1} \exp(-y) dy = \theta^b x^b \int_0^1 w^{b-1} \exp(-\theta x w) dw,$$

where the change of variable $w = y/(\theta x)$ was considered. Analogously,

$$\gamma(c, \xi x) = \xi^c x^c \int_0^1 u^{c-1} \exp(-\xi x u) du.$$

Hence,

$$\begin{aligned} \int_0^\infty x^{a-1} \exp(-sx) \gamma(b, \theta x) \gamma(c, \xi x) dx \\ = \theta^b \xi^c \int_0^\infty \int_0^1 \int_0^1 [x(s+\theta w+\xi u)]^{a+b+c-1} \exp[-x(s+\theta w+\xi u)] \frac{w^{b-1} u^{c-1}}{(s+\theta w+\xi u)^{a+b+c-1}} dw du dx. \end{aligned}$$

Making the change of variable $z = x(s+\theta w+\xi u)$ and changing the order of integration, the last integral becomes

$$\begin{aligned} &= \theta^b \xi^c \int_0^1 \int_0^1 \left[\int_0^\infty z^{a+b+c-1} \exp(-z) dz \right] \frac{w^{b-1} u^{c-1}}{(s+\theta w+\xi u)^{a+b+c}} dw du \\ &= \theta^b \xi^c \Gamma(a+b+c) \int_0^1 \int_0^1 \frac{w^{b-1} u^{c-1}}{(s+\theta w+\xi u)^{a+b+c}} dw du. \end{aligned}$$

By changing w to $1-w$ and u to $1-u$, the above integral can be written as

$$= \frac{\theta^b \xi^c \Gamma(a+b+c)}{(s+\theta+\xi)^{a+b+c}} \int_0^1 \int_0^1 \frac{(1-w)^{b-1} (1-u)^{c-1}}{\left(1 - \frac{\theta}{s+\theta+\xi} w - \frac{\xi}{s+\theta+\xi} u\right)^{a+b+c}} dw du.$$

In short, we have proven that

$$\int_0^\infty x^{a-1} \exp(-sx) \gamma(b, \theta x) \gamma(c, \xi x) dx = \frac{\theta^b \xi^c \Gamma(a+b+c)}{(s+\theta+\xi)^{a+b+c}} \int_0^1 \int_0^1 \frac{(1-w)^{b-1} (1-u)^{c-1}}{\left(1 - \frac{\theta}{s+\theta+\xi} w - \frac{\xi}{s+\theta+\xi} u\right)^{a+b+c}} dw du. \quad (36)$$

By using in (36) the well-known integral representation of the Appell F2 double hypergeometric function:

$$\begin{aligned} & F_2(a, b_1, b_2; c_1, c_2; x, y) \\ &= \frac{\Gamma(c_1)\Gamma(c_2)}{\Gamma(b_1)\Gamma(b_2)\Gamma(c_1-b_1)\Gamma(c_2-b_2)} \int_0^1 \int_0^1 u^{b_1-1} v^{b_2-1} (1-u)^{c_1-b_1-1} (1-v)^{c_2-b_2-1} (1-ux-vy)^{-a} du dv, \end{aligned}$$

the proof follows. \square

Proposition A.3. The following identity is valid

$$\int_0^\infty x^{a-1} \exp(-sx) \gamma(b, \theta x) dx = \frac{\theta^b \Gamma(a+b)}{b(s+\theta)^{a+b}} {}_2F_1\left(a+b, 1; b+1; \frac{\theta}{s+\theta}\right),$$

where $a > 0$, $s > 0$, $\theta > 0$ and $b > 0$.

Proof. By taking $c = 1$ and then $\xi \rightarrow \infty$ in (36), we get

$$\begin{aligned} \int_0^\infty x^{a-1} \exp(-sx) \gamma(b, \theta x) dx &= \lim_{\xi \rightarrow \infty} \frac{\theta^b \xi \Gamma(a+b+1)}{(s+\theta+\xi)^{a+b+1}} \int_0^1 \int_0^1 \frac{(1-w)^{b-1}}{\left(1 - \frac{\theta}{s+\theta+\xi} w - \frac{\xi}{s+\theta+\xi} u\right)^{a+b+1}} dw du \\ &= \lim_{\xi \rightarrow \infty} \theta^b \Gamma(a+b) \int_0^1 (1-w)^{b-1} \left\{ (s+\theta-\theta w)^{-a-b} - (s+\theta+\xi-\theta w)^{-a-b} \right\} dw \\ &= \frac{\theta^b \Gamma(a+b)}{(s+\theta)^{a+b}} \int_0^1 (1-w)^{b-1} \left(1 - \frac{\theta}{s+\theta} w\right)^{-a-b} dw. \end{aligned} \quad (37)$$

By using in (37) the well-known integral representation of the hypergeometric function:

$$\mathbf{B}(b, c-b) {}_2F_1(a, b; c; z) = \int_0^1 x^{b-1} (1-x)^{c-b-1} (1-zx)^{-a} dx, \quad c > b > 0,$$

the proof readily follows. \square

Remark A.4. We point out that an erroneous formula for the integral of the lower incomplete gamma of Proposition A.3 with $\theta = 1$ has appeared in D'Aurizio (2016).